INVESTIGATION OF SOURCE POINT INSTABILITIES IN DIPOLE MAGNET BASED BEAMLINES

M. Apollonio, Diamond Light Source, Oxfordshire, U.K.
R. Bartolini, Diamond Light Source, Oxfordshire, U.K. and
John Adams Institute, University of Oxford, U.K.

Abstract

At Diamond the source point in the second dipole of the Double Bend Achromats (DBA) can vary due the lack of adjacent BPMs constraining angle and position of the electron beam at the dipole. We have implemented a code based on our AT model to predict the effects of a corrector strength change and compared our predictions to data both from a beamline and from our pinhole cameras. We discuss the possibility of interfacing the code to a ray tracing routine in order to infer beam spot changes in the downstream beamline and suggest a procedure to restore the original source point.

INTRODUCTION

In the Diamond Storage Ring (SR) there are 48 dipole magnets and provision for the same number of beamline front-ends. 22 front-ends are available for synchrotron light created by insertion devices in the straights, and 24 for synchrotron light generated in dipoles (BM front-ends and beamlines). Each Bending Magnet (BM) produces 131 mrad of synchrotron radiation, of which 35 mrad get into the entrance of every BM front-end. For standard BM front-ends there is a further cut-off to 20 mrad, while special BM front-ends use non-standard designs to capture all the 35 mrad horizontal radiation. These BM lines include infra-red (IR) and circular dichroism (CD) beamlines. In the CD lines, a combination of a flat and a toroidal mirror is utilized to create a point to point optics.

SOURCE POINT INSTABILITIES

B23 is a dipole beamline for circular dichroism studies [1]. The beam of synchrotron light is steered through a mirror based optical system that focuses the source point onto an image plane, where the main instrumentation is located (see Fig. 1). The photons from the source point (SP) first meet a flat mirror (M1) at a vertical grazing angle of 15°, then a toroidal mirror (M2) with the same inclination and finally another flat mirror (M3) set at 45° with respect to the upcoming beam. M3 can be moved vertically at different heights, partially intersecting the beam and letting light go towards station A and station B with different intensities. For the purpose of this study we will consider M3 in the upper position, with the beam reaching only station B. At the image plane, a slit of variable aperture is placed. Its possible values are reported on Tab. 1 together with the main characteristics of the beamline. Occasional variations in the photon signal intensity, typically occurring after shut-downs, were observed in the B23 experimental hut.

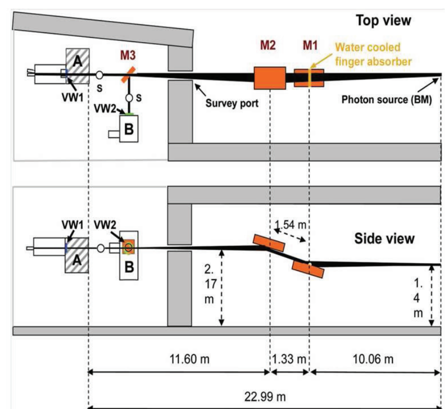

Figure 1: Schematic of B23 from [1].The source point is transported 1:1 to the image plane.

Table 1: B23 beamline parameters from [1] and [2]

mirror	type	size (mm)	grazing angle	slit size at image plane
M1	planar	400x280	15°	H=
M2	toroidal $R1_{mer}$=44.8m $r2_{sag}$=3m	460x310	15°	[0.125, 0.200, 0.280, 0.500, 1.000] (mm)
M3	planar	160x30	45°	V=10.0 (mm)

The actual location of the sixth corrector magnet in a cell (CM(6)) can cause a bump in the orbit between the beam positions monitors BPM(5) and BPM(6), determining both a shift and a tilt in the beam at the nominal source point position (10.69 cm inside the BM). A matlab script using AT for tracking was developed to investigate the issue. The code finds the track compatible with the optics of the machine and the readings from the BPMs in the region around dipole 2. As shown in Fig. 2 (top), a trajectory of an electron is never flat when CM(6) is active, even if the orbit passes through the zeros of the nearby BPMs. Both SP shift and trajectory inclination exhibit a linear dependence from CM(6) current (Fig. 2 (bottom)). In both planes CM(6) values can vary from one run to another, due to changes occurring during shut-downs. The aforementioned tracking script allows to identify a SP shift of about 20 μm related to a current change of 0.62 A at HCM(6) occurred between RUN1 and RUN2 (2012), when the problem was highlighted by the B23 team [3]. In order to assess the extent of these shifts on the real set-up (both machine and

ISBN 978-3-95450-122-9

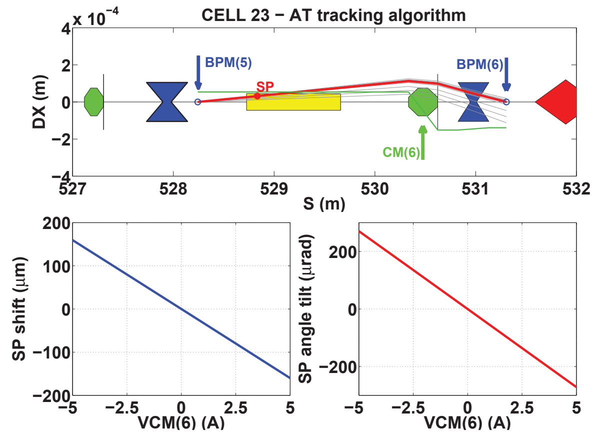

Figure 2: Effect of CM(6) non zero current for an orbit passing through the zeros of BPM(5) and BPM(6). (Top) orbit as calculated by a tracking algorithm, (bottom) dependence on CM(6) current for SP (left) and for the orbit inclination (right).

B23 beamline) a test was carried over on July 17$^{\text{th}}$ 2012.

B23 Beam Spot Test

For this test CM(6) in cell 23 is disabled from the Fast Orbit Feed Back system (FOFB) and its current is varied in both planes. The tracking script calculates the SP shift and tilt inside the dipole using the actual positions recorded at BPM(5) and BPM(6) and the current at CM(6). The corresponding shift in the beam spot at B23 is recorded for every corrector current. Horizontal and Vertical excitations of CM(6) were scanned separately. For the measurement B23 modified its apparatus at station B by inserting a CCD camera device at the location usually occupied by the vertical slit (*i.e.* the image plane). A snapshot of the photon beam from the CCD camera is shown in Fig. 3.

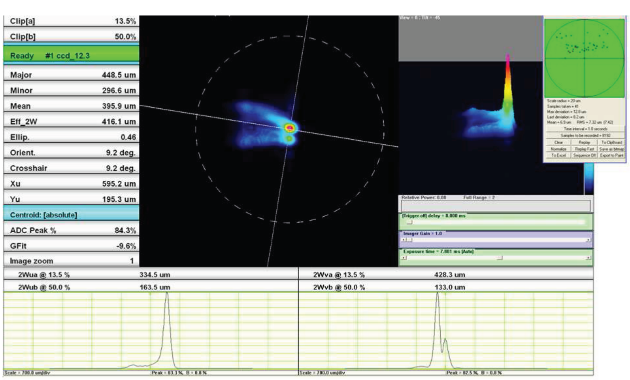

Figure 3: B23 beam image on a CCD camera. The beam spot size is H=163 μm and V=133 μm (FWHM) with clear non gaussian features.

Results are summarized in Table 2. The measured shift per Ampere is comparable in both planes, and the SP shift predictions are close to the values observed in B23. This is consistent with a 1:1 optics for the system. If we take

Table 2: Results of the test conducted at B23 to measure beam spot movements as a function of CM(23,6) current.

	beam spot at B23 image plane (μm)	SP inside dipole 2 (μm)	ΔI_{CM6} (A)	gradient (μm/A)
Δx	43.2±7.5	44.65	1.48	29±5
Δy	34.2±2.0	35.87	1.26	27±2

Δx/ΔI= 29 μm/A as a figure, we expect a source displacement of 18 μm for the case reported by the beamline. An attempt to assess the effect of such a movement on the beam spot at B23 is reported in the next paragraphs.

Pin Hole Camera Test

The robustness of our SP tracking code was tested using one of the Pin Hole (PH) camera devices usually utilized to determine the emittance of the beam. The PH test shows a very good agreement between data and model, strengthening our confidence in B23 results (see Fig. 4 (left))

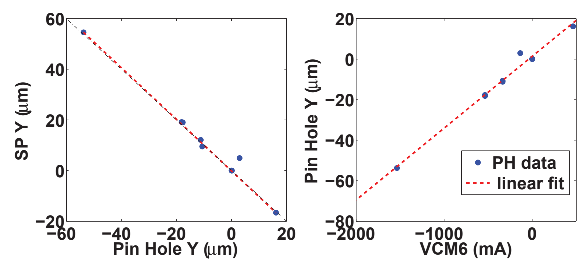

Figure 4: Pin hole camera test. (Left) tracking algorithm reconstructed SP versus PH camera data. (Right) PH camera points versus VCM(6) current.

Ray Tracing of B23

A shift (and tilt) of the original source can move the image totally or partially out of the physical aperture (slit) of the measuring device, causing a clipping of the impinging light and determining a potentially important reduction in intensity as reported by B23. A plain ray tracing calculation based on the code SHADOW3 [4] has been used in order to better understand the implications of a movement in the SP. As a future application one may think of a combined use of the e-beam tracking script and SHADOW3 to give a quick prediction of image movements due to SP instabilities for different beamline optical systems. Fig. 5 shows a rendering of the B23 optical system, whose main parameters are taken from [1][2], where a point-like source shoots rays with a typical $1/\gamma$ gaussian emission resulting in a point-like beam spot at the nominal image plane. Horizontal shifts of the SP, correctly reproduced at the image plane, are the most important effect to be taken into account whereas the beamline results nearly insensitive to the angular movements of the SP.

For the case under study, approximating the real beam with a gaussian of $\sigma_H = 69.4\,\mu$m that interpolates the main horizontal peak from Fig. 3 we can infer that $\delta \mathrm{I}_{CM(6)}$ =

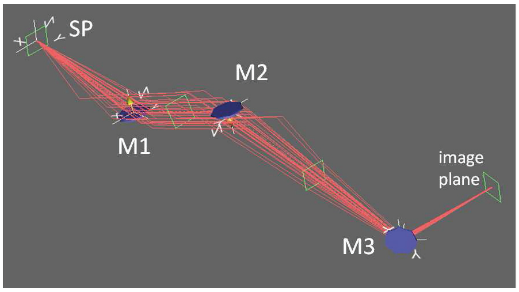

Figure 5: SHADOW3 rendering of the ray tracing in the B23 optical system. The initial point-like source is transported to a point-like image. The M1 flat, M2 toroidal and M3 flat mirrors are clearly visible. Note the logarithmic scale compressing the main length of the system (about 23m).

0.62A generating a 18 μm drift out of the slit would cause a maximal reduction of 20% of the initial signal, if the initial beam is peaking at the edge of the slit before the change occurs (see Fig. 6).

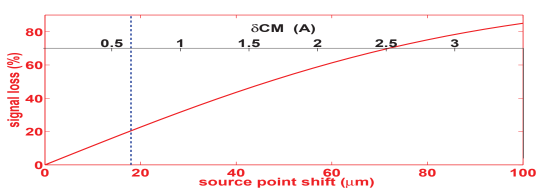

Figure 6: Signal reduction for a gaussian beam spot initially sitting at the edge of a slit.

A GOLDEN OFFSET FEEDBACK FOR SP RESTORING

Excluding CM(6) from the feedback system and locking its current to a reference value is a non viable option since it reduces the effectiveness of the orbit corrections, especially if this solution has to be applied to all the BM lines. We devised another possibility based on changes in the Golden Offset (GO) at BPM(6) (GO(6)), such way we can restore the original SP. Using the AT model we defined a test to verify this option. GO(7) is deliberately altered in order to produce a distorted orbit, while the FOFB is kept active. The beam is forced to pass through the zero of the BPMs while the new orbit generates a well defined change in the SP. CMs react to this perturbation in a perfectly predictable way. The restoring algorithm defines the GO at step n as:

$$
\begin{aligned}
\delta(SP)_n &= SP_n - SP_{n-1} \\
\delta(GO)_n &= -0.015[\mathrm{mm}]/7.4[\mu\mathrm{m}] \cdot \delta(SP)_n \\
GO_n &= GO_{n-1} + \delta(GO)_n \cdot \alpha
\end{aligned} \quad (1)
$$

where $\alpha = [0.4, 1.6]$ ensures a convergence in less than 10 iterations. Fig. 7 shows the result of a test conducted on Diamond SR cell 1. The top plot illustrates the changes in SP position, from the tracking code, and the corresponding PH camera output. Iteration 0 corresponds to the unperturbed system. When GO(7) is changed to 100 μm at iteration 1 the FOFB reacts by generating a change in the orbit between BPM(5) and BPM(6). From iteration 2 on we see the restoring feedback system in action. Three steps after perturbation are needed to bring the system back to the initial SP value. A good matching between PH camera points and tracking algorithm predictions is observed. The bottom picture shows a remarkable agreement between data and model for the CMs involved in the test.

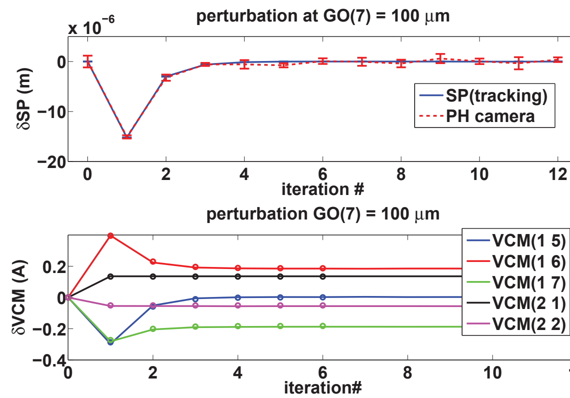

Figure 7: (Top) tracked SP variation (blue) versus PH camera output (red).(Bottom) CM variations for correctors involved in the test, both for measured values (lines) and as predicted by model (circles).

CONCLUSIONS

Tests conducted in collaboration with a Diamond BM beamline (B23) have shown a clear correlation between beam spots changes at the beamline and current variation in one of our corrector magnets. This is confirmed in our model, with remarkable agreement. An initial study based on an optical ray tracing code has shown how a first estimate of signal loss can be given. A feedback system meant to restore the original SP after a change in CM(6) has been succesfully tested at the Diamond Storage Ring.

ACKNOWLEDGMENTS

We wish to thank G. Siligardi and T. Javorfi for their collaboration in the test at B23, C. Thomas for his advice on the use of PH cameras, L. Alianelli for discussions on SHADOW3 and G. Rehm for initially suggesting Golden Offsets to correct for SP instabilites.

REFERENCES

[1] G. Siligardi *et al.* in BLS-B23-REP-0002 (A) (Diamond Internal Report).

[2] “Report for B23”, BLS-B23-REP-0003, (Diamond Internal Report).

[3] G. Rehm, G. Siligardi *private communication*.

[4] M. Sanchez del Rio *et. al.*, in J. of Synchrotron Radiation, 2011, Sept 1,18(Pt 5): 708-716

ISBN 978-3-95450-122-9